# Elliptical jet breakup related with the internal nozzle flow

Jung Goo Hong*†, Kun Woo Ku *and Choong Won Lee* and Byung Chul Na**

* Department of Mechanical Engineering
Kyungpook National University
1370 Sankyuk-dong Buk-gu, Daegu, Republic of Korea

**Energy System Research Center
Korea Automotive Technology Institute
303 Pungse-myeon, Dongnam-gu, Chonan-si, Republic of Korea

**Abstract**

An experimental study was conducted to investigate the atomization characteristics of a circular nozzle and elliptical nozzles of small diameter (0.5mm) under the high injection pressure (1MPa~9MPa). Furthermore, numerical simulations were attempted to investigate the internal flow structure in the circular and elliptical nozzles. This study showed that the disintegration characteristics of the liquid jet of elliptical nozzles were much different from those of the circular nozzle. In the case of the circular nozzle, the surface of liquid jet was much smooth near the nozzle exit under the injection pressures of this study. But, in the case of the elliptical nozzles, surface waves on liquid jet have been generated and grown with increase of the injection pressure. As a result, surface breakup was observed with the increase of injection pressure because a rough column surface caused by growth of surface wave is disintegrated to ligament as the relative velocity between the liquid jet and ambient air increases. Furthermore, the numerical simulations informed that the internal flow structure of elliptical nozzle was quite different from that of the circular nozzle. The internal flow structure of the elliptical nozzle in hydraulic flip was reattached to the orifice wall of the minor axis unlike the flow in the circular nozzle which is detached from orifice wall. It has been concluded that the internal flow structure of the elliptical nozzle has influence on the disintegration characteristics of the liquid jet issued from the elliptical nozzle.

## Introduction

Recently, many researchers reported that the primary breakup of a liquid jet is greatly influenced by the cavitating flow in the orifice. Most of the previous studies primarily focused on axi-symmetrical nozzles. But the studies on asymmetrical jets, such as the jets produced by elliptic nozzles, have been steadily increased, although these studies have received little attention. Especially, the characteristics of an elliptic spray are quite different to those of a circular spray. Jacobsson et al.[1] and Yuny et al.[2]observed axis-switching and concluded that spray cone angles and the spread were larger in the minor axis plane than in the major axis plane. Kasyap et al. [3,4] conducted an experimental study on a liquid jet discharging from an elliptical orifice. They reported that the axis-switching of the elliptical nozzle is strongly dependent upon the aspect ratio (a/b) of an orifice as well as the viscosity of the liquid and that it improves liquid jet break up. According to the above studies, the spray characteristics of an elliptical nozzle are admittedly better than those of a circular nozzle and that the cavitating flow in the orifice influences atomization performance. Recently, Hong et al.[5] carried out an experimental study to investigate the cavitating flow of elliptical nozzles and circular nozzle. They reported that the cavitation in the circular nozzle had a cylindrical shape which was symmetrical to the nozzle's axis, but that the cavitation shape in the elliptical nozzles had a horseshoe-like shape whose cavitation length in the major axis plane was longer than that in the minor axis plane. Furthermore, Hong et al.[6] conducted a numerical simulation to investigate cavitating flow characteristics in an elliptical nozzle by using a full cavitation model in the CFD code FLUENT 6.2. These previous studies on an elliptical nozzle are divided into three parts. First, an elliptical nozzle was applied to the diesel injector. In the case of a diesel injector, it is not been made clear on the cause of the atomization characteristics on an elliptical nozzle because the injection velocity of the liquid jet is high relatively. Second, the breakup length was measured under relatively low injection pressure for a large hole diameter nozzle. Third, the internal flow was investigated by using a transparent nozzle and CFD code. Unfortunately, these studies were conducted for a large hole diameter nozzle under relatively low injection pressure. For these reasons, it is difficult to define the atomization mechanism of an elliptical nozzle through these studies. Therefore, we

†Corresponding author: jghong70@knu.ac.kr

carried out an experimental study on the atomization characteristics of an elliptical nozzle with a small hole diameter (0.5mm) and under relatively high injection pressure (1MPa~9MPa). We thought that the atomization characteristics of an elliptical nozzle were related to the internal flow structure characteristics in the orifice. Thus, we carried out a numerical study to investigate the internal flow structure in an elliptical nozzle. We used the results from these studies to clarify the atomization mechanism of an elliptical nozzle and to identify the relationship between the internal flow structure characteristics and the atomization characteristics.

**Experimental Methods**

Figure 1 illustrates the experimental setup, which consists of an injection device, visualization system and pressure measurement. Working fluid was water at room temperature. The water pressurized by nitrogen in the surge tank was injected from the nozzle into ambient air. The nozzle was linked to the traverse for movement. Injection pressure was controlled by the pressure of the nitrogen gas, which was controlled by the gas regulator. Injection pressures were measured by a pressure transducer (KELLER, PA-21SR). The pressure signals were acquired by data acquisition board and monitored in real time. The spray image was obtained by the shadowgraph method using a CCD camera (Vieworks, VM-2M 35) and a xenon lamp (Drello, Drelloscope 3020) as the light source. The spray images were automatically stored by the image grabber, which was interlinked with the computer. The macroscopic characteristics of the liquid jet were analysed from the spray images. Furthermore, flow rate was measured with the mass cylinder for one minute. Flow rate was the mean value of 20 measured values. The discharge coefficient ($C_d$) was computed by

$$C_d = \frac{Q}{A\sqrt{2\Delta P_i/\rho}} \quad (1)$$

where A is cross-sectional area of the orifice, Q is flow rate, $\Delta P_i$ represents the pressure difference between the upstream and downstream of test nozzle and ambient pressure and ρ is liquid density. The atomization characteristics of elliptical nozzles were compared with that of one circular nozzle under the same experimental condition. Figure 2 illustrates the circular nozzle and elliptical nozzles used in this study. The cross-sectional areas of all nozzles were approximately the same based on a 0.5mm diameter circular nozzle. The length-to-diameter ratios (ℓ/D) of all nozzles were 4. The geometric details of the nozzles are given in Table 1. The experimental conditions are given in Table 2.

**Numerical Methods and Grid Generation**

We carried out a numerical study to investigate the internal flow characteristics of an elliptical nozzle by using the commercial CFD software FLUENT 6.2. The working fluid is assumed to be a mixture of liquid, vapor and non-condensable gases. Standard governing equation in the mixture model and in mixture turbulence model describes the flow and account for turbulence. The vapor transport equation governs the vapor mass fraction, $f_v$ by the following equation:

$$\frac{\partial}{\partial t}(\rho_m f_v) + \nabla(\rho_m \vec{v}_v f_v) = \nabla(\gamma \nabla f_v) + R_e - R_c \quad (2)$$

where $\rho_m$ is mixture density, v is the velocity vector of the vapor, γ is the effective exchange coefficient, and Re and $R_c$ are the vapor generation and condensation rate terms. The density of mixture, $\rho_m$, can be calculated as

$$\rho_m = \alpha_v \rho_v + \alpha_g \rho_g + (1 - \alpha_v - \alpha_g)\rho_l \quad (3)$$

where the subscripts v, g and l represent vapor, non-condensable gas and liquid, respectively, and $\alpha_v$, $\alpha_g$, and $\alpha_l$ are the respective volume fractions. The relationship between the mass fraction (f) and the volume fraction (α) are related as

$$\alpha_v = f_v \frac{\rho_m}{\rho_v}, \qquad \alpha_g = f_g \frac{\rho_m}{\rho_g}, \text{ and } \quad \alpha_l = f_l \frac{\rho_m}{\rho_l} \quad (4)$$

The rate terms are derived from the Rayleigh-Plesset equations, and limiting bubble size considerations. These rates are functions of the instantaneous, local static pressure and can be expressed as

$$R_e = C_e \frac{\sqrt{k}}{\sigma} \rho_l \rho_v \sqrt{\frac{2(p_{sat} - p)}{3\rho_l}} (1 - f_v - f_g) \quad \text{when} \quad p < p_{sat} \quad (5)$$

$$R_c = C_c \frac{\sqrt{k}}{\sigma} \rho_l \rho_l \sqrt{\frac{2(p - p_{sat})}{3\rho_l}} f_v \quad \text{when} \quad p > p_{sat} \quad (6)$$

where σ is the surface tension of the liquid, $p_{sat}$ is the liquid saturation vapor pressure at the given temperature, and p and k are static pressure and local turbulence intensity, respectively. Also $C_e$ and $C_c$ are empirical constants. The default $C_e$ and $C_c$ values are 0.02 and 0.01. FLUENT's cavitation model accounts for the turbulence-induced pressure fluctuations by simply raising the phase-change threshold pressure from $p_{sat}$ to

$$p_v = \frac{1}{2}(p_{sat} + p_{tur}) \quad (7)$$

where $P_{turb}$=0.39ρk. The source and sink terms in eq. (5 and 6) are obtained from the simplified solution of the Rayleigh-Plesset equation [6-9]. Grid generation for the computational domain and specifications for circular and elliptical nozzles are shown in Figure 3. A mesh in the computational domain was generated by using

GAMBIT. A high density mesh was generated for the orifice, where cavitation is actually generated, by creating a boundary layer in the GAMBIT. The boundary conditions and properties of the working fluid are shown in the Table 3.

## Results and Discussion

### 1. Discharge coefficient with injection pressure

In this study, the discharge coefficient is shown in Figure 4. Hong et al.[5] reported that the discharge coefficient has a constant value regardless of nozzle geometry if hydraulic flip occurs in the orifice. Song et al. [10] conducted experimental study using a circular nozzle with a hole diameter (0.5mm) and length to diameter (ℓ/d=5). They reported that the discharge coefficient value remains constant although the pressure difference increases when hydraulic flip occurs. Furthermore, the specification of circular nozzle in this work was same as the nozzle used by Tamaki et al.[11] According to their result, hydraulic flip in the orifice is generated above the injection pressure of 0.24MPa in their experiment using this nozzle. Even the lowest injection pressure of this work is much higher than 0.24MPa. From the results of these studies, we can deduce that the internal flow condition is the hydraulic flip in experimental conditions of this work although the internal flow condition is not observed directly from an experiment.

### 2. Disintegration characteristics of liquid jet

This study was conducted to investigate the atomization characteristics a circular nozzle and elliptical nozzles with different aspect ratios (a/b). The images of liquid jets emanating from the test nozzles are presented in Figure 5. These images were captured from the nozzle exit to 15mm of the nozzle downstream. In the case of the circular nozzle, the liquid jet had a smooth surface with increase of injection pressure. Furthermore, the main liquid jet was not disintegrated with injection pressure although droplets were observed around the circumference of the issuing jet. As mentioned above, in the hydraulic flip regime of the circular nozzle, the liquid flow that separated at the nozzle inlet does not reattach to the nozzle wall. In this case, cavitation disappears because the downstream air occupies the space between the nozzle wall and liquid flow. As a result, the liquid flow in the orifice is enveloped by the downstream air and the liquid jet has a very smooth surface. The disintegration characteristics of the liquid jet in the circular nozzle investigated in this work were similar to those of previous works for the disintegration of liquid jet in the hydraulic flip regime. However, in the case of the elliptical nozzles, the disintegration characteristics of the liquid jet were much different from that of the circular nozzle. As shown in Figure 5, the liquid jet issued from the elliptical nozzles became more wrinkled at the same injection pressure than that of the circular nozzle. In other words, the surface waves on the liquid jets issued from the elliptical nozzles have been more clearly observed at 1MPa of injection pressure unlike that of the circular nozzle. Moreover, surface breakup was observed at the jets issued from the elliptical nozzles with the increase of injection pressure because a rough column surface caused by growth of surface wave is disintegrated to ligament as the relative velocity between the liquid jet and ambient air increases. We thought that the liquid jet issued from the elliptical nozzles is more wrinkled unlike that the circular nozzle due to the internal flow structure.

### 3. Internal flow structure of the elliptical nozzle

The internal flow structure in nozzle with a small hole diameter is difficult to investigate by experiment. Hence, a numerical simulation using CDF code FLUENT 6.2 was carried out to investigate the internal flow structure. We referred to the boundary conditions of Tafreshi et al.[12]who have conducted the numerical simulations for the hydraulic flip using FLUENT. Furthermore, we referred to the numerical simulation model and conditions validated by Hong et al.[6] who carried out the numerical simulation of the internal flow for an elliptical nozzle using FLUENT 6.2. Figure 6 shows the flow structure in the orifice for the simulation nozzles. In the case of the circular nozzle, the internal flow structure was similar to the hydraulic flip of literature, in which the distribution of cavitation reached at nozzle outlet is symmetrical to the orifice circumference. Also, there was no significant difference of the internal flow structure with the increase of injection pressure. However, the internal flow structure of elliptical nozzle was quite different from that of the circular nozzle. As shown in the front view of orifice outlet of E2 nozzle in Figure 6, the cavitation reaches the orifice outlet from the both sides of the major axis plane but at the minor axis plane, liquid is full under the injection conditions of this work. At that time, the cavitation-filled space is filled with downstream air. This flow structure is referred to as the hydraulic flip of the elliptical nozzle. As appears by Figure 6, regardless of the injection pressure, the flow detached from the orifice wall at the circular nozzle and the major axis plane of elliptical nozzle, but the flow at the minor axis plane reattached to the orifice wall. These results can explain how a disintegration of liquid jet is promoted in an elliptical nozzle. Figure 7 shows the disintegration mechanism of liquid jet issued from an elliptical nozzle in the hydraulic flip regime. As shown in Figure 7, in the hydraulic flip regime, the flow detaches from the orifice wall of the

circular nozzle In this case, the surface roughness of the orifice wall does not affect the flow and the jet is constricted by the ambient air. Thus, the liquid jet has a smooth surface. However, in the case of the elliptical nozzle, the flow reattaches to orifice wall of the minor axis plane although the flow is detached from the orifice wall of the major axis plane. In this case, the liquid jet can be unstable and dispersed because the wall friction effect such as flow perturbation caused by shear flow between the flow and orifice wall and a flow separation caused by flow structure are both present [13-16]. For this reason, it is thought that the disintegration of liquid jet issued from the elliptical nozzle can be promoted when compared to that of the circular nozzle as shown in Figure 5.

**Summary and Conclusions**

The atomization mechanism of an elliptical nozzle was studied by experiments. The atomization characteristics of the elliptical nozzle in this study were related to the internal flow structure characteristics in the orifice. Hence, the internal flow structure in the elliptical nozzle was investigated by numerical study using the full cavitation model in the CFD code FLUENT 6.2. The conclusions are as follows

(1) In the hydraulic flip regime, the discharge coefficient was constant, regardless of the injection pressure. The difference of discharge coefficient did not appear with the aspect ratio of the nozzle.

(2) In the case of the circular nozzle, the disintegration characteristic of liquid jet in the hydraulic flip regime was similar to those of previous works. However, in the case of the elliptical nozzles, the disintegration characteristic of the liquid jet was much different from that of the circular nozzle. The surface waves on the liquid jets issued from the elliptical nozzles have been more clearly observed at 1MPa of injection pressure unlike that of the circular nozzle. Moreover, surface breakup was observed at the jets issued from the elliptical nozzles with the increase of injection pressure because a rough column surface caused by wrinkled liquid jet is disintegrated to ligament as the relative velocity between the liquid jet and ambient air increases.

(3) In the case of the elliptical nozzle, regardless of the injection pressure, the flow in the orifice detached from the orifice wall at the major axis plane, but the flow at the minor axis plane reattached to the orifice wall. From these results, the liquid jet issued from the elliptical nozzle can be unstable and dispersed because the wall friction effect such as flow perturbation caused by shear flow between the flow and orifice wall and a flow separation caused by the flow structure are both present.

**Acknowledgements**

This work was supported by Priority Research Centers Program through the National Research Foundation of Korea (NRF) funded by the Ministry of Education, Science and Technology (2011-0018392).

**References**

[1] Jacobsson, L., Winklhofer, E., and Chomiak, J., *SAE Tech. Pap. Ser.*, 1999-01-3490 (1999)
[2] Yunyi, G., Changwen, L., Yezhou, H., and Zhijun, P., *SAE Tech. Pap. Ser*., 982546 (1998)
[3] Kasyap, T. V., Sivakumar, D., and Raghunandan, B. N., *Atomization Sprays 18*: 645-668, (2008)
[4] Kasyap, T. V., Sivakumar, D., and Raghunandan, B. N., *International Journal of Multiphase Flow 35*: 8-19 (2009)
[5] Hong, J. G., Ku, K. W., Kim, S. R., and Lee, C. W., *Atomization Sprays 20*: 877-886 (2010)
[6] Hong, J. G., Ku, K. W., and Lee, C. W., *Atomization Sprays 21*: 237-248 (2011)
[7] Singhal, A. K., Athavale, M. M., Huiying, L., and Jiang, Y., *ASME Journal of Fluids Engineering 124*: 617-624 (2002)
[8] Som, S., Aggarwal S. K., EI-Hannouny, E. M., and Longman, D. E., *ASME Journal of Engineering for Gas Turbines and Power 132-4*: 042802 (2010)
[9] Fluent Inc, *Fluent user's guide volume 3, Fluent Inc*: 22.1-22.96 (2003)
[10] Song, J. K., Ahn, K. B., Kim, M. K., and Yoon, Y. B., *Journal of Propulsion and Power 27*: 608-619 (2011)
[11] Tamaki, N., Shimizu, M., Nishida, K., and Hiroyasu, H., *Atomization Sprays 8*: 179-197 (1998)
[12] Tafreshi, H. V., and Pourdeyhimi, H., *Textile Research Journal 74*: 359-364 (2004)
[13] Birouk, M., and Lekic, N., *Atomization Sprays 19*: 501-528 (2009)
[14] Christophe, D., *Experiments in Fluids 45-3*: 271-422 (2008)
[15] Hiroyasu, H., *Atomization Sprays 10*: 511-517 (2000)
[16] McCarthy, M. J., and Molloy, N. A., *Chemical Engineering Journal 7*:1-20 (1974)

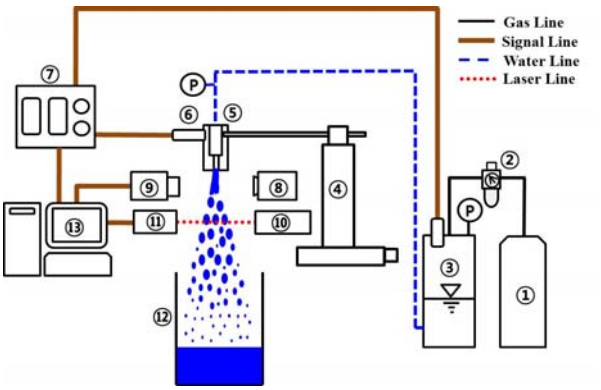


**Fig. 1** Schematic diagram of the experimental setup. (1) $N_2$ gas; (2) gas regulator; (3) surge tank; (4) traverse;(5) test nozzle; (6) pressure transducer; (7) data acquisition board; (8) strobe scope; (9) CCD camera; (10) laser for SMD; (11) detector; (12) mass cylinder; (13) computer

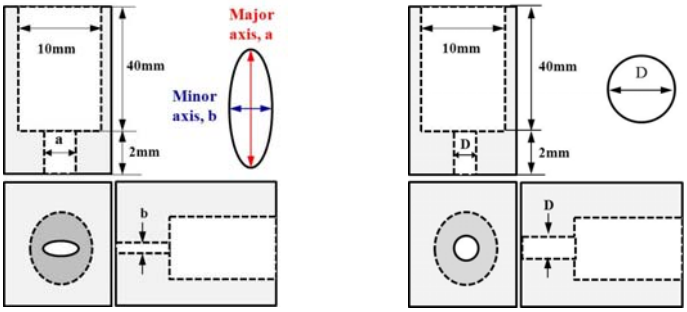


(a) Elliptical nozzle (b) Circular nozzle

**Fig. 2** Schematic diagram of the test nozzles, (a) Elliptical nozzle (b) Circular nozzle

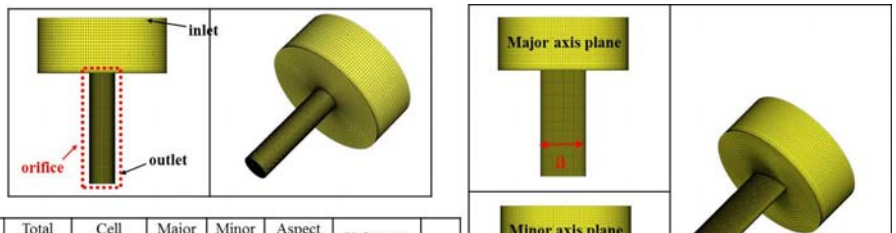


| | Total cell number | Cell number of orifice | Major axis, a (mm) | Minor axis, b (mm) | Aspect ratio, a/b | Hole area, A (mm²) | ℓ/d |
|---|---|---|---|---|---|---|---|
| C | 702,993 | 522,003 | 0.5 | 0.5 | 1 | 0.2 | 4 |
| E2 | 730,304 | 526,400 | 0.7 | 0.35 | 2 | 0.2 | 4 |

**Fig. 3** Grid generation of the computational domain and specifications for the simulation nozzles

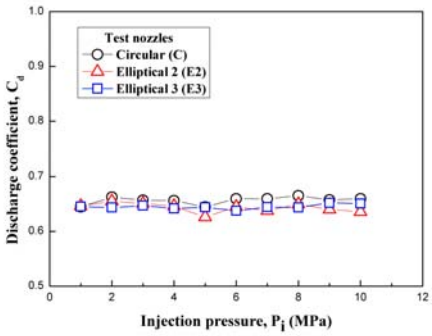


**Fig. 4** Discharge coefficient with injection pressure

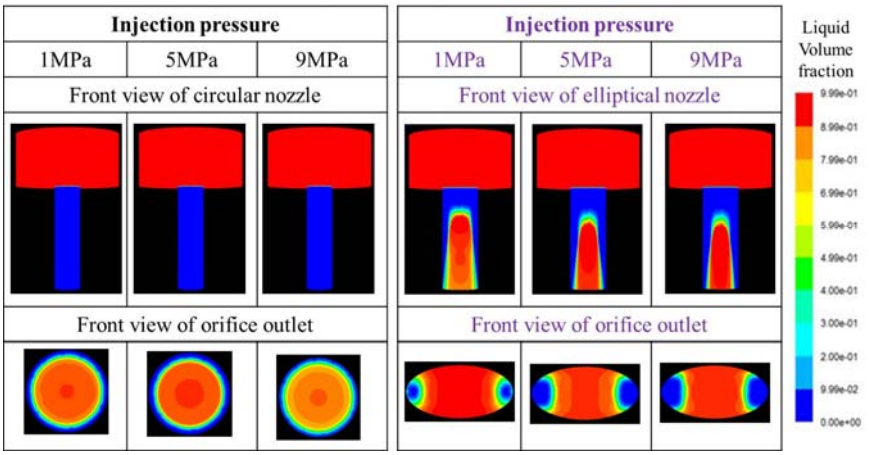


**Fig. 6** Flow structure in the orifice for the simulation nozzles

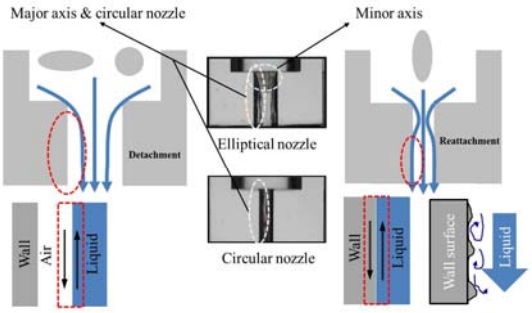


**Fig.7** Disintegration mechanism of liquid jet issued from the elliptical nozzle in the hydraulic flip regime (Internal flow images from Hong et al. (2010))

Table 1 Geometrical detail and experimental conditions

| Item / Test nozzles | Major axis, a (mm) | Minor axis, b (mm) | Circumference (mm) | Aspect ratio, a/b | Area, A ($mm^2$) |
|---|---|---|---|---|---|
| Circular(C) | 0.5 | 0.5 | 3.007 | 1 | 0.20 |
| Elliptical 2 (E2) | 0.705 | 0.375 | 2.768 | 1.9 | 0.21 |
| Elliptical 3 (E3) | 0.9 | 0.31 | 2.543 | 2.9 | 0.22 |

Table 2 Experimental condition

| | | |
|---|---|---|
| Working fluid | Water | |
| Injection pressure (MPa) | 1 ~ 9 | |
| Physical properties of working fluid | Temperature (°C) | 27 |
| | Density ($kg/m^3$) | 1000 |
| Ambient pressure (MPa) | 0 | |

Table 3 Boundary conditions and fluid property for simulation

| | | |
|---|---|---|
| Working fluid | Water | |
| Inlet pressure (MPa) | 1, 5, 9 | |
| Property of fluid | Temperature (℃) | 27 |
| | Density ($kg/m^3$) | 1000 |
| | Viscosity ($N·s/m^2$) | $1\times10^{-3}$ |
| | Liquid surface tension (N/m) | 0.0717 |
| | Vapor pressure ($N/m^2$) | 3540 |
| Outlet pressure (MPa) | 0 | |

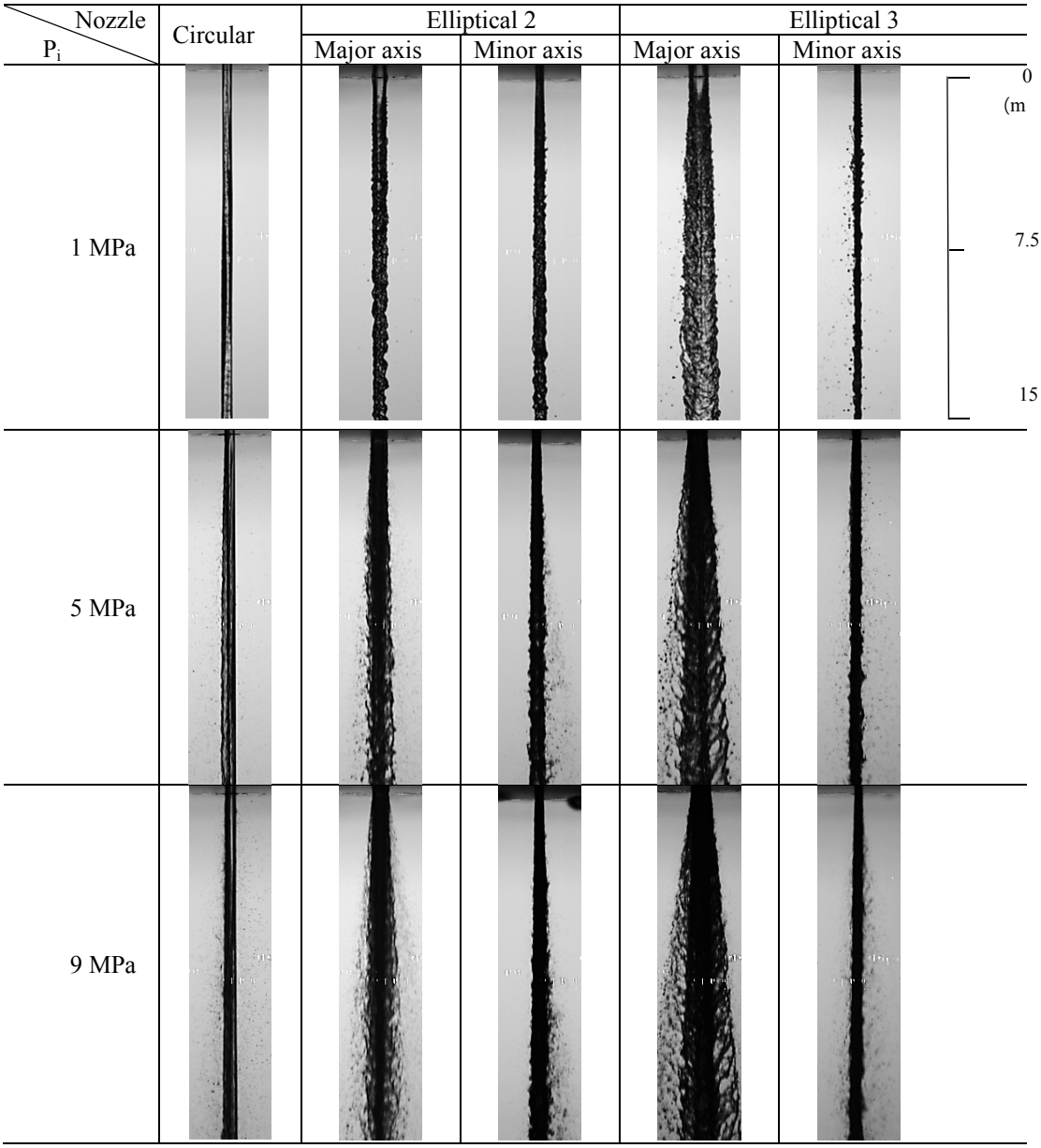


Fig. 5 Effect of the nozzle geometry on disintegration of the liquid jets